H_2 Sensing Properties of Diode-type Gas Sensors
Fabricated with Ti- and/or Nb-based Materials

Takeo Hyodo[1],*, Hiroki Shibata[1], Yasuhiro Shimizu[2], and Makoto Egashira[2]

[1]Graduate School of Science and Technology, Nagasaki University

[2]Department of Materials Science and Engineering, Faculty of Engineering, Nagasaki University

1-14 Bunkyo-machi, Nagasaki 852-8521, Japan

*Corresponding author:

Takeo Hyodo, Dr.

Graduate School of Science and Technology, Nagasaki University

1-14 Bunkyo-machi, Nagasaki 852-8521, Japan

Tel: +81-95-819-2645

Fax: +81-95-819-2643

E-mail: hyodo@nagasaki-u.ac.jp

Abstract

A thermally oxidized TiO_2 or Nb_2O_5 film equipped with a top Pd film electrode and a bottom Ti or Nb plate electrode (Pd/MO(n)/M, MO: oxide film, M: metal plate, n: annealing temperature (°C)) has been investigated as a diode-type H_2 sensor under air or N_2 atmosphere. Pd/TiO_2(n)/Ti sensors showed relatively poor H_2 sensing properties in air, in comparison with Pd/anodic-TiO_2(n)/Ti sensors constructed with an anodized TiO_2 film equipped with a top Pd film electrode and a bottom Ti plate electrode, which were reported in our previous studies. On the other hand, Pd/Nb_2O_5(n)/Nb sensors showed relatively larger H_2 response with fast response and recovery speeds than Pd/TiO_2(n)/Ti sensors in air under high forward bias conditions. A Pd/Nb_2O_5(450)/Ti sensor, which was fabricated by radio-frequency magnetron sputtering of Nb metal on a Ti substrate followed by thermal oxidation at 450°C, showed the largest H_2 response and relatively fast response and recovery speeds in air, among the sensors tested. In addition, H_2 response of the Pd/Nb_2O_5(450)/Ti sensor in air was much lower than that in N_2, but the logarithm of H_2 response was almost proportional to the logarithm of H_2 concentration in a wide range of H_2 concentration (10~8000 ppm) in air, and the H_2 sensitivity in air was much higher than that in N_2.

Keywords: Gas sensor, Hydrogen, Titania, Niobium oxide, Palladium

1. Introduction

Recently, numerous efforts have been directed to developing various kinds of H_2 sensors [1-6], because H_2 gas as a clean energy source is significantly expanding into various fields. We also reported various diode-type H_2 sensors with high and reversible H_2 response as well as fast response and recovery behavior in both air and N_2 atmospheres, compared with other types of gas sensors [7-13]. These diode-type sensors (Pd/anodic-TiO_2(n)/Ti, MO: TiO_2 or Nb_2O_5, M: Ti or Nb, n: annealing temperature (°C)) were fabricated by anodic oxidation of a metal plate (Ti or Nb) and then consisted of thin metal oxide films (TiO_2 or Nb_2O_5) having well-developed macropores at their surface and noble metal electrodes (mainly Pd). Their excellent H_2 sensing properties seem to arise from much lower Schottky barrier height at the boundary between the Pd electrode and the oxide film in H_2 than that in air, due to dissociative adsorption of H_2 molecules and subsequent dissolution of H atoms into the Pd electrode. On the other hand, Lee et al. reported that a TiO_2 film which was fabricated by thermal oxidation of a Ti plate can also become an attractive H_2 sensing material by controlling the fabrication conditions strictly [14].

In this study, therefore, thin metal oxide films (TiO_2 or Nb_2O_5) on Ti or Nb plates were fabricated under different conditions by utilizing thermal oxidation and/or radio-frequency (rf) magnetron sputtering, and H_2 sensing properties of these films coupled with a Pd electrode were investigated under both air and N_2 atmospheres.

2. Experimental

A Ti or Nb metal plate (5.0×5.0 mm^2) with a thickness of 0.5 mm was oxidized thermally in air at 600~900°C for 6 h or 400~550°C for 1 h, respectively. In some cases, a Nb thin film was physically deposited on the surface of the Ti plate by rf magnetron sputtering (Shimadzu Emit Co., Ltd., HSR-552S) at 300 W for 5 min, and it was also heat-treated at 450°C for 6 h in air. Back sides of these samples were polished by an emery paper to eliminate any oxide layers to ensure the following electrical contacts. The samples obtained were referred to as MO(n)/M (M: Ti or Nb, MO: TiO_2 or Nb_2O_5, n: annealing temperature (°C)). The microstructure of the oxide films prepared was observed by a scanning electron microscope (SEM; Hitachi, Ltd., S-2250N).

A palladium thin film was sputtered at 300 W for 10 min on the surface of the oxidized films, and then Au wires were attached with a Pd paste (Tanaka Kikinzoku Kogyo K.K., T60) on both sides of the samples. Thereafter, they were fired at 400°C for 1 h in air. The MO(n)/M coupled with a Pd electrode was represented as Pd/MO(n)/M.

A dc voltage of +0.04~1.0 V was applied to the Pd/MO(n)/M under the forward bias conditions, i.e. Pd(+)/MO/M(-), and transient changes in current flowing through the sensors upon exposure to 10~8000 ppm H_2 balanced with dry air or nitrogen were monitored at 200~300°C, by employing a potentiostat (Solartron Analytical, 1287A). The response measurement was conducted in a flow apparatus at a gas flow rate of 100 cm^3 min^{-1}. The volume from the switch valve for changing the gas flowing to the installation position of a sensor was about 90 ml in the present flow apparatus. Therefore, the time necessary for complete substitution for gaseous environment over the sensor is estimated to be more than 1 min under the present experimental conditions. Current(I)-voltage(V) characteristics of the sensors were also measured in a range of -2.0~2.0 V at a sweep rate of 10 mV s^{-1} by employing the potentiostat. The magnitude of sensor response was defined as I_g-I_b, where I_g and I_b represented a sensor current in 10~8000 ppm H_2 balanced with air or N_2 and in a base gas (air or N_2), respectively.

3. Results and Discussions

3.1 Characterizations of TiO$_2$(n)/Ti and H$_2$ sensing properties of Pd/TiO$_2$(n)/Ti sensors

Figure 1 shows XRD patterns of Ti plates thermally oxidized in air at 600~900°C for 6 h (TiO$_2$(n)/Ti). Small peaks of rutile and anatase phases were observed for TiO$_2$(600)/Ti, together with those expected of a Ti phase. The fraction of the rutile phase increased obviously when the Ti plate was heated at 700°C, and the anatase phase could not be confirmed at heating temperatures higher than 800°C. SEM photographs of the surface of TiO$_2$ films thermally oxidized at temperatures higher than 700ºC are shown in Fig. 2. The TiO$_2$ film in the TiO$_2$(600)/Ti was too thin, and therefore its image was not clearly observed by SEM. A typically dense TiO$_2$ film with large agglomerates (1.5~2.0 μm wide, ≤ 6.0 μm long) was formed at the surface of a Ti plate after the heating at 700°C (TiO$_2$(700)/Ti), and a certain number of small particles with a diameter of less than 0.2 μm also existed on the large agglomerates. In addition, grain-boundaries were very obscure. On the other hand, the sizes of both agglomerates and small particles increased with an increase in the annealing temperature (agglomerates: 2.5~6.0 μm wide and ≤ 8.0 μm long for TiO$_2$(800)/Ti, ≤ 9.0 μm wide and ≤ 20 μm long for TiO$_2$(900)/Ti; small particles: ≤ 0.5 μm for TiO$_2$(800)/Ti, ≤ 1.0 μm for TiO$_2$(900)/Ti in diameter). No submicron-size open pores were observed on the TiO$_2$ surface of all TiO$_2$(n)/Ti plates, although many disordered and well-developed macropores (50~130 nm in diameter) were formed at the surface of the anodized TiO$_2$ films [7-12].

Figure 3 shows I-V characteristics in air and in 8000 ppm H_2 balanced with air of

Pd/TiO$_2$(n)/Ti sensors at 300°C.　Response transients of these sensors to 8000 ppm H$_2$ in air at a forward bias voltage of 0.1 V at 300°C are shown in Fig. 4.　Pd/TiO$_2$(600)/Ti showed almost metallic conductivity and then was not suitable for a sensor material, probably due to a very thin TiO$_2$ film on the Ti Plate (the data is not shown here).　The I-V curve of the Pd/TiO$_2$(700)/Ti sensor in air showed ohmic behavior with relatively large current, and its non-linearity was observed in 8000 ppm H$_2$ balanced with air under a forward bias. Accordingly, the base current in air was also too high even at +0.1 V, as shown in Fig. 4(a). The response speed to 8000 ppm H$_2$ of the Pd/TiO$_2$(700)/Ti sensor in air was typically fast, but the serious problem was too large over-shooting behavior.　Currents both in air and in 8000 ppm H$_2$ balanced with air observed with the Pd/TiO$_2$(900)/Ti sensor were extremely low and it showed no response to H$_2$, probably because of the formation of an extremely thick TiO$_2$ film on the surface of the Ti plate.　On the other hand, the Pd/TiO$_2$(800)/Ti sensor showed much better non-linear I-V characteristics under a forward bias, based on the Schottky barrier at the Pd/TiO$_2$ interface, among the Pd/TiO$_2$(n)/Ti sensors tested.　It also showed the most stable H$_2$ response among them, but the H$_2$ sensing properties (especially, H$_2$ response and recovery behavior) was inferior to those of the H$_2$ sensors fabricated with anodized TiO$_2$ films (Pd/anodic-TiO$_2$(n)/Ti) reported in our previous studies (the magnitude of sensor response (I_g-I_b): ca. 5 x 10^{-2} mA even at 250°C) [7-12].　The fast response and recovery of the anodized TiO$_2$ film is undoubtedly attributed to its porous structure which facilitates H$_2$ gas diffusion into the interface between Pd and TiO$_2$.　And therefore slow response and recovery behavior of the Pd/TiO$_2$(800)/Ti is then considered to arise from its dense TiO$_2$ film.

3.2 Characterizations of Nb$_2$O$_5$(n)/Nb and H$_2$ sensing properties of Pd/Nb$_2$O$_5$(n)/Nb sensors

Nb metal was generally less stable in air at elevated temperatures than Ti metal.　Thus, a Nb$_2$O$_5$ film on the Nb plate was prepared by heating at lower temperatures for shorter times than the conditions necessary for the formation of a TiO$_2$ film from a Ti plate as described above.　Figures 5 and 6 show XRD patterns and SEM photographs of thermally oxidized Nb$_2$O$_5$ films in air at 400~550°C for 1 h (Nb$_2$O$_5$(n)/Nb).　Nb$_2$O$_5$(400)/Nb showed no diffraction peaks except for those of Nb metal (Fig. 5(a)), but a little amount of products (submicron-size agglomerates with submicron-size particles) were observed at the surface of the Nb plate (Fig. 6(a)).　Clear diffraction peaks expected for Nb$_2$O$_5$ were confirmed after the Nb metal was heat-treated in a temperature range between 450°C and 550°C.　Their

surface morphology was extremely rough and little dependent on their annealing temperature. In addition, it was largely different from that of an anodized Nb_2O_5 film with disordered macropores (ca. 1~3 μm in diameter), as reported previously [13].

Figure 7 shows I-V characteristics in air and in 8000 ppm H_2 balanced with air of the $Pd/Nb_2O_5(n)/Nb$ sensors at 200°C. Response transients of these sensors to 8000 ppm H_2 in air at a forward bias voltage of 0.1 V at 200°C are shown in Fig. 8. $Pd/Nb_2O_5(400)/Nb$ could not be used as a diode-type gas sensor, because its resistance was too low. However, $Pd/Nb_2O_5(450)/Nb$ showed a non-linear I-V characteristic and a large current in 8000 ppm H_2 under forward bias conditions, while the current in air was extremely small even at a forward bias voltage of 2.0 V, as shown in Fig. 7(a). As a result, a large response to 8000 ppm H_2 was induced at a forward bias voltage of 1.0 V, as shown in Fig. 8(a). On the other hand, $Pd/Nb_2O_5(500)/Nb$ and $Pd/Nb_2O_5(550)/Nb$ also showed clear difference in I-V characteristics between in air and in 8000 ppm H_2 balanced with air, as shown in Figs. 7(b) and 7(c), but the heat-treatment above 500°C resulted in too high sensor resistance and too small magnitude of response, as shown in Figs. 8(b) and 8(c). Figure 9 shows cross-sectional SEM photographs of $Nb_2O_5(n)/Nb$ (n = 450, 500 and 550). The Nb_2O_5 films consisted of stacked layers with a thickness of several μm, and the thickness of the Nb_2O_5 films (i.e., the number of stacked layers) increased with an increase in heating temperature. The resistance of diode-type gas sensors is generally dependent only on the magnitude of Schottky barrier formed at the metal/oxide interface. However, the resistance of $Pd/Nb_2O_5(n)/Nb$ sensors seems to be largely influenced by the thickness of the Nb_2O_5 film. Therefore, strict thickness-control of the Nb_2O_5 film is indispensable in order to utilize the Nb_2O_5 as a diode-sensor material, but the thermal instability of the Nb metal apparently prohibits the improvement on the electrical and gas-sensing properties of $Pd/Nb_2O_5(n)/Nb$ sensors.

3.3 Characterizations of $Nb_2O_5(n)/Ti$ and H_2 sensing properties of $Pd/Nb_2O_5(n)/Ti$ sensors

A Nb film was deposited on a Ti plate by rf magnetron sputtering at 300 W for 5 min, and then heat-treated at 450°C for 6 h in air, to fabricate a thin Nb_2O_5 film on the thermally stable Ti plate. SEM photographs of the thin Nb_2O_5 film fabricated on the Ti plate are shown in Fig. 10. The dense Nb_2O_5 film with a relatively smooth surface and a well-controlled thickness (ca. 0.7 μm) was observed on the Ti plate, in comparison with $Nb_2O_5(n)/Nb$ (see Figs. 6 and 9). The $Pd/Nb_2O_5(450)/Ti$ sensor showed excellent nonlinearity of I-V curves at 100°C and 250°C as well as a large difference in sensor current between in air and in 8000

ppm H_2 balanced with air under a forward bias condition, as shown in Fig. 11, and thus it was expected that such I-V characteristics would guarantee much better responses to H_2. H_2 response transients of the Pd/Nb_2O_5(450)/Ti sensor at 100°C and 250°C in air are shown in Fig. 12. The sensor exhibited a much larger H_2 response and faster response and recovery speeds at 250°C than Pd/TiO_2(n)/Ti and Pd/Nb_2O_5(n)/Nb sensors. In addition, a clear H_2 response was confirmed even at 100°C, while the response and recovery speeds at 100°C became slower than those at 250°C, probably because H atoms dissolved in the Pd metal were not easily released to air at 100°C. H_2 sensing properties of the Pd/Nb_2O_5(450)/Ti sensor in N_2 were also measured at 100°C and 250°C, as shown in Fig. 13. The magnitude of H_2 responses in N_2 was more than ten times larger than that in air both at 100°C and 250°C, while the recovery speed in N_2 was much slower than that in air. Our previous study showed that the recovery speed of Pd/anodic-TiO_2(n)/Ti sensors under N_2 atmosphere was terribly slower than that under air atmosphere, probably because the H atoms absorbed in the Pd metal under N_2 atmosphere were slowly desorbed as H_2 molecules from the Pd surface and those absorbed in the Pd metal under air atmosphere were quickly desorbed as H_2O molecules from the Pd surface after reacting with O_2 [12]. The difference of such H_2-desorption behavior between in air and in N_2 may also have a great influence on the recovery behavior of the Pd/Nb_2O_5(450)/Ti sensor, as shown in Figs. 12 and 13.

Figure 14 shows variations of H_2 response of the Pd/Nb_2O_5(450)/Ti sensor with H_2 concentration in air and in N_2. The logarithm of H_2 response of the sensor operated under a forward bias voltage of 0.4 V was almost proportional to the logarithm of H_2 concentration in the wide range of H_2 concentration (10~8000 ppm) in air. In addition, a clear H_2 response (ca. 2 μA) and fast response and recovery behavior (not shown here) were confirmed even to 10 ppm H_2 in air. This may promise that the sensor can detect H_2 in the concentration range of ppb level in air. In contrast, the responses to more than 500 ppm H_2 in N_2 were much larger than those in air, even under an extremely low applied voltage of 0.01 V, but the responses to H_2 less than 100 ppm in N_2 were not confirmed at all. In addition, the H_2 sensitivity (the slope of the linear relationship between $\log(I_g-I_a)$ and $\log(H_2$ concentration)) in N_2 was also smaller than that in air. The mechanism of such incomprehensible behavior in N_2 is not clear at present, but the surface reactivity and the solubility of H_2 into Pd and the variation in work function of Pd as a function of H_2 concentration in N_2 may be involved in such behavior.

4. Conclusion

H$_2$ sensing properties of Pd/MO(n)/M (MO: TiO$_2$ or Nb$_2$O$_5$, M: Ti or Nb, n: annealing temperature (°C)) as a diode-type gas sensor were investigated under air or N$_2$ atmosphere. The H$_2$ responses of Pd/TiO$_2$(n)/Ti sensors fabricated in this study were inferior to those of Pd/anodic-TiO$_2$(n)/Ti sensors reported in our previous studies, under air atmosphere [7-12]. On the other hand, Pd/Nb$_2$O$_5$(n)/Nb sensors, which were operated under a high forward bias voltage of +1.0 V, showed better H$_2$ sensing properties in air than Pd/TiO$_2$(n)/Ti sensors. However, the resistance of the Nb$_2$O$_5$ film was too high and the Nb metal was thermodynamically instable at elevated temperatures for gas-sensor applications. A Pd/Nb$_2$O$_5$(450)/Ti sensor showed the largest H$_2$ response and relatively fast response and recovery speeds in air among the sensors tested. The H$_2$ response of the Pd/Nb$_2$O$_5$(450)/Ti sensor in air was much lower than that in N$_2$ in the concentration range of more than 500 ppm, but it showed a clear H$_2$ response with relatively fast response and recovery speeds in a wide H$_2$ concentration range of 10~8000 ppm in air.

References

1. K. Sahner and H. L. Tuller, Novel deposition techniques ofr metal oxide: Prospects for gas sensing, J. Electroceram. (2008), doi10.1007/s10832-008-9554-7 (available online).

2. G. K. Mor, O. K. Varghese, M. Paulose, K. Shankar, and C. A. Grimes, A review on highly ordered, vertically oriented TiO$_2$ nanotube arrays: material properties, and solar energy applications, Sol. Energy Mater. Sol. Cells, 90 (2006) 2011-2075.

3. E. Comini, C. Baratto, G. Faglia, M. Ferroni, A. Vomiero, and G. Sberveglieri, Quasi-one dimensional metal oxide semiconductors: Preparation, characterization and application as chemical sensors, Prog. Mater. Sci., 54 (2009) 1-67.

4. I.-D. Kim, A. Rothschild, T. Hyodo, and H. L. Tuller, Microsphere templating as means of enhancing surface activity and gas sensitivity of CaCu$_3$Ti$_4$O$_{12}$ thin films, Nano Lett., 6 (2006) 193-198.

5. T. Hyodo, N. Nishida, Y. Shimizu, and M. Egashira, Preparation and gas-sensing properties of thermally stable mesoporous SnO$_2$, Sens. Actuators B, 83 (2002) 209-215.

6. T. Hyodo, S. Abe, Y. Shimizu, and M. Egashira, Gas sensing properties of ordered mesoporous SnO$_2$ and effects of coatings thereof, Sens. Actuators B, 93 (2003) 590-600.

7. Y. Shimizu, N. Kuwano, T. Hyodo, and M. Egashira, High H$_2$ sensing performance of anodically oxidized TiO$_2$ film contacted with Pd, Sens. Actuators B, 83 (2002) 195-201.

8. T. Iwanaga, T. Hyodo, Y. Shimizu, and M. Egashira, H$_2$ sensing properties and mechanism of anodically oxidized TiO$_2$ film contacted with Pd Electrode, Sens.

Actuators B, 93 (2003) 519-525.

9. T. Hyodo, T. Iwanaga, Y. Shimizu, and M. Egashira, Effects of electrode materials and oxygen partial pressure on the hydrogen sensing properties of anodically oxidized titanium dioxide films, ITE Lett., 4 (2003) 594-597.

10. H. Miyazaki, T. Hyodo, Y. Shimizu, and M. Egashira, Hydrogen-sensing properties of anodically oxidized TiO_2 film sensors: Effects of preparation and pretreatment conditions, Sens. Actuators B, 108 (2005) 467-472.

11. Y. Shimizu, K. Sakamoto, M. Nakaoka, T. Hyodo, and M. Egashira, H_2 sensing performance of TiO_2-based diode-type sensors, Adv. Mater. Res., 47-50 (2008) 1510-1513.

12. M. Nakaoka, T. Hyodo, Y. Shimizu, and M. Egashira, Hydrogen sensing properties of an anodized TiO_2 film equipped with a Pd-Pt electrode, ECS Transactions, 16(11), edited by R. Mukundan, Z. Aguilar, C. Bruckner-Lea, M. Carter, G. Hunter, N. Miura, F. Mizutani, and Y. Shimizu (2008) 317-323.

13. T. Hyodo, J. Ohoka, Y. Shimizu, and M. Egashira, Design of anodically oxidized Nb_2O_5 films as a diode-type H_2 sensing material, Sens. Actuators B, 117 (2006) 359-366.

14. Y.-K. Jun, H.-S. Kim, J.-H. Lee, and S.-H. Hong, High H_2 sensing behavior of TiO_2 films formed by thermal oxidation, Sens. Actuators B, 107 (2005) 264-270.

Biographies

Takeo Hyodo received his B. Eng. Degree in applied chemistry and M. Eng. Degree in materials science and technology in 1992 and 1994, respectively, and Dr. Eng. Degree in 1997 from Kyushu University. He has been an Assistant Professor at Nagasaki University since 2007. His research interests are the developments of electrochemical devices such as chemical sensors and lithium batteries, and mesoporous and macroporous materials.

Hiroki Shibata received his B. Eng. Degree and M. Eng. Degree in materials science and engineering from Nagasaki Uniersity in 2004 and 2006, respectively.

Yasuhiro Shimizu received his B. Eng. Degree in applied chemistry in 1980 and Dr. Eng. Degree in 1987 from Kyushu University. He has been a Professor at Nagasaki University since 2005. His current research concentrates on development of odor sensors and design of intelligent sensors by controlling gas diffusivity and reactivity.

Makoto Egashira received his B. Eng. Degree and M. Eng. Degree in applied chemistry in 1966 and 1968, respectively, and Dr. Eng. Degree in 1974 from Kyushu University. He has been a Professor at Nagasaki University since 1985. His current interests include the development of new chemical sensors, surface modification of ceramics, preparation of hollow ceramic microspheres and porous films and application of microwave-induced plasma.

Figure Captions

Fig. 1.   XRD patterns of Ti plates thermally oxidized in air at 600~900°C for 6 h (TiO$_2$(n)/Ti, n: (a) 600, (b) 700, (c) 800 and (d) 900).

Fig. 2.   SEM photographs of thermally oxidized TiO$_2$ films of TiO$_2$(n)/Ti (n: (a) 700, (b) 800 and (c) 900).

Fig. 3.   I-V characteristics of Pd/TiO$_2$(n)/Ti sensors (n: (a) 700, (b) 800 and (c) 900) in air (solid line) and in 8000 ppm H$_2$ balanced with air (dashed line) at 300°C.   *: the bias voltage applied when the response behavior of the sensors was measured.

Fig. 4.   Response transients to 8000 ppm H$_2$ in air of Pd/TiO$_2$(n)/Ti sensors (n: (a) 700, (b) 800 and (c) 900) at 300°C.

Fig. 5.   XRD patterns of Nb plates thermally oxidized in air at 400~550°C for 1 h (Nb$_2$O$_5$(n)/Nb, n: (a) 400, (b) 450, (c) 500 and (d) 550).

Fig. 6.   SEM photographs of thermally oxidized Nb$_2$O$_5$ films of Nb$_2$O$_5$(n)/Nb (n: (a) 400, (b) 450, (c) 500 and (d) 550).

Fig. 7.   I-V characteristics of Pd/Nb$_2$O$_5$(n)/Nb sensors (n: (a) 400, (b) 450, (c) 500 and (d) 550) in air (solid line) and in 8000 ppm H$_2$ balanced with air (dashed line) at 200 °C. *: the bias voltage applied when the response behavior of the sensors was measured.

Fig. 8.   Response transients to 8000 ppm H$_2$ in air of Pd/Nb$_2$O$_5$(n)/Nb sensors (n: (a) 400, (b) 450, (c) 500 and (d) 550) at 200°C.

Fig. 9.   Cross-sectional SEM photographs of Nb$_2$O$_5$(n)/Nb (n: (a) 450, (b) 500 and (c) 550).

Fig. 10. SEM photographs of Nb$_2$O$_5$(450)/Ti fabricated by rf magnetron sputtering of Nb on a Ti plate, followed by heat-treatment at 450°C for 5 h.

Fig. 11. I-V characteristics of a Pd/Nb$_2$O$_5$(450)/Ti sensor in air (solid line) and in 8000 ppm H$_2$ balanced with air (dashed line) at 100 and 250°C.   *: the bias voltage applied when the response behavior of the sensors was measured.

Fig. 12. Response transients of a Pd/Nb$_2$O$_5$(450)/Ti sensor to 8000 ppm H$_2$ in air under a

forward bias voltage of 0.4 V at 100 and 250ºC.

Fig. 13. Response transients of a Pd/Nb$_2$O$_5$(450)/Ti sensor to 8000 ppm H$_2$ in N$_2$ under a forward bias voltage of 0.01 V at 100 and 250ºC.

Fig. 14. Relationship between H$_2$ response of a Pd/Nb$_2$O$_5$(450)/Ti sensor and H$_2$ concentration in air and in N$_2$ at 250ºC.
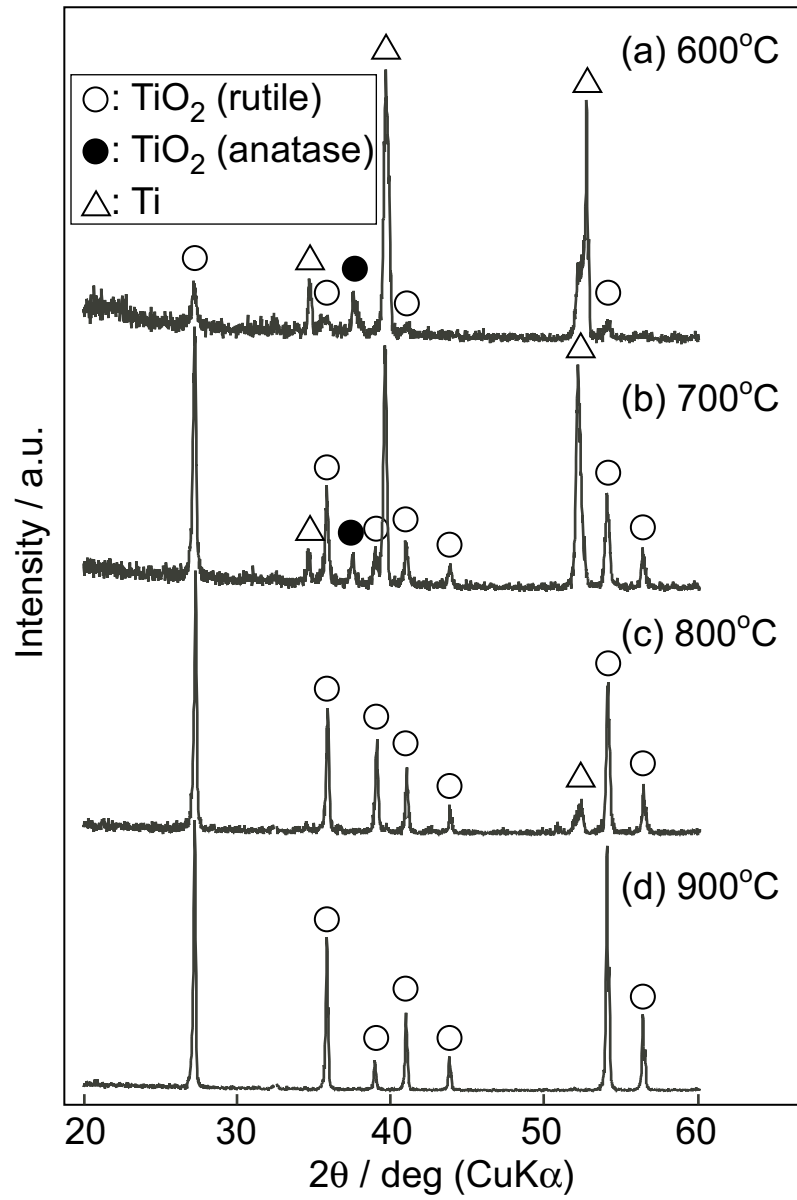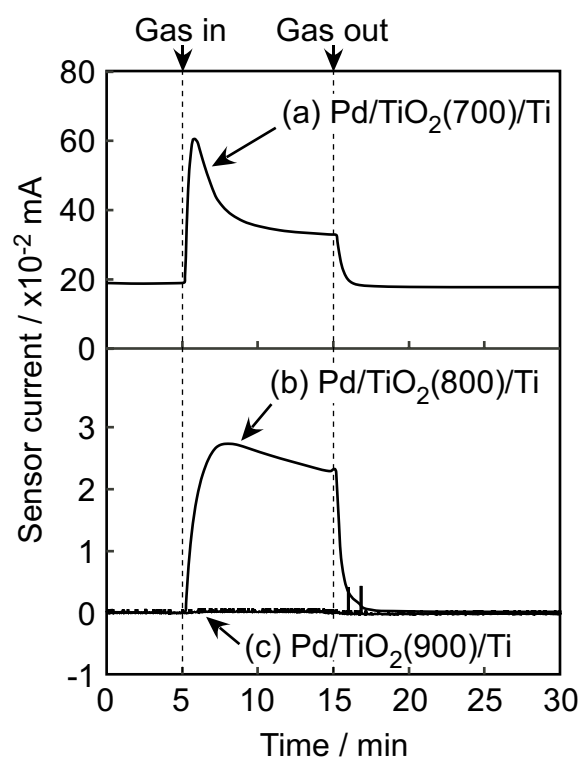
Fig. 1.   Hyodo et al.

(a) 700°C

5.0 μm

(b) 800°C

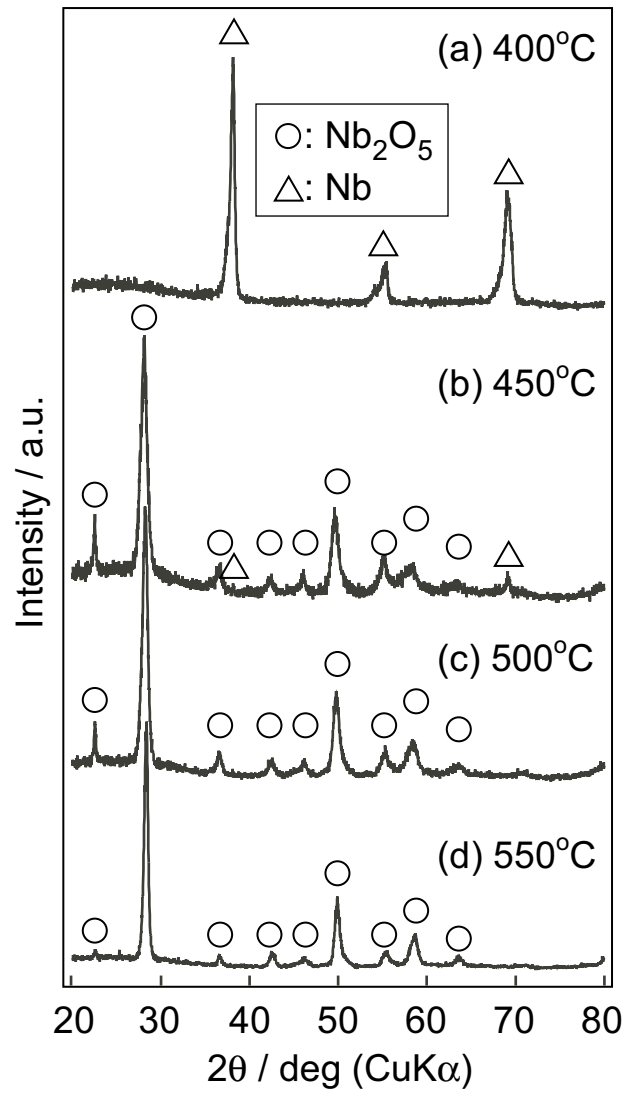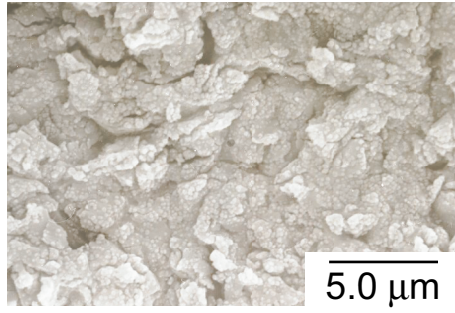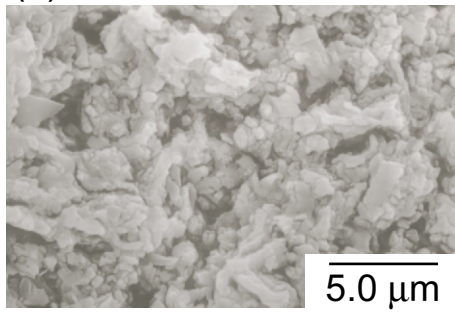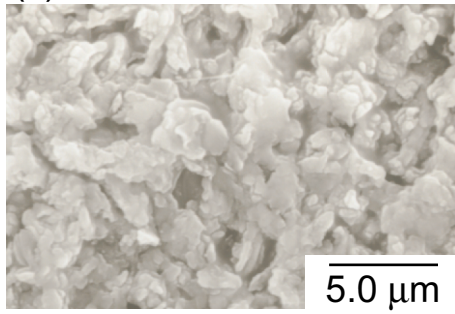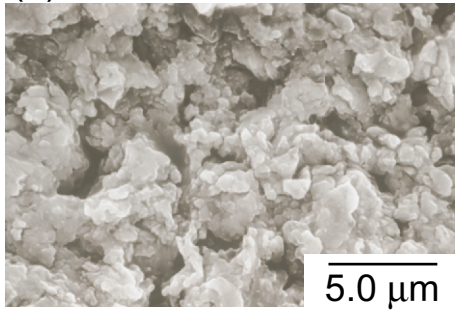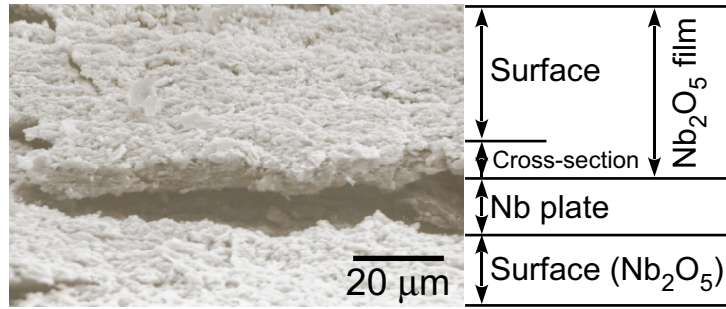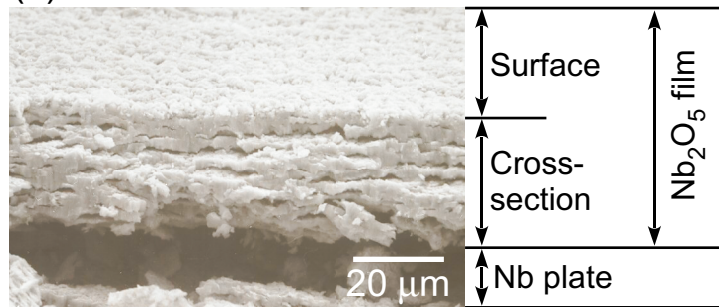5.0 μm

(c) 900°C

5.0 μm
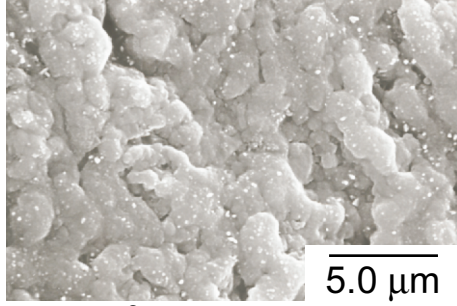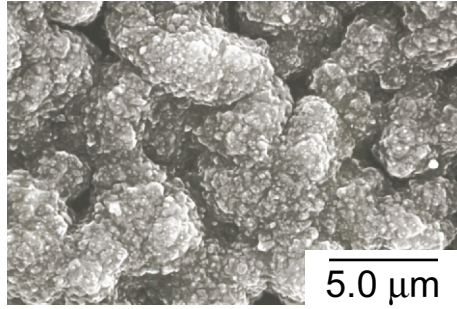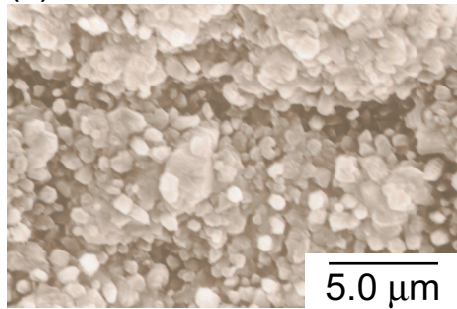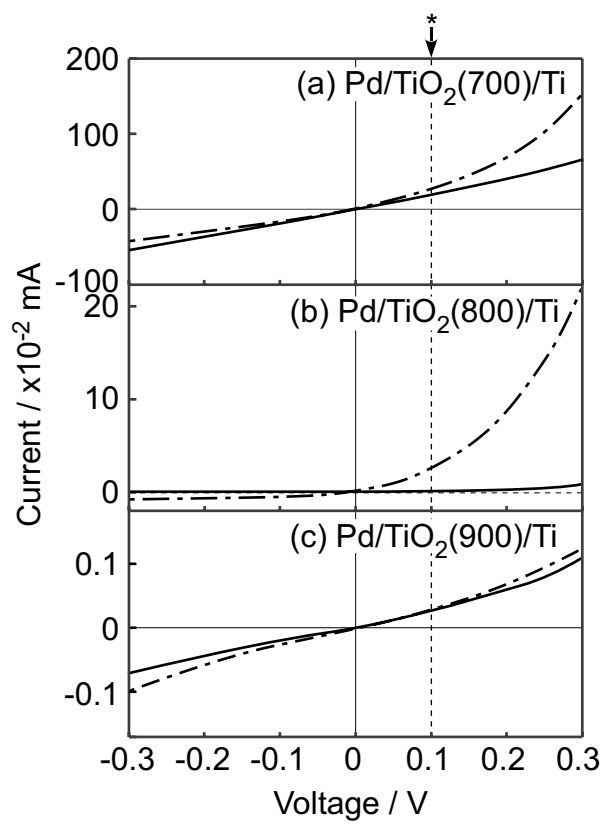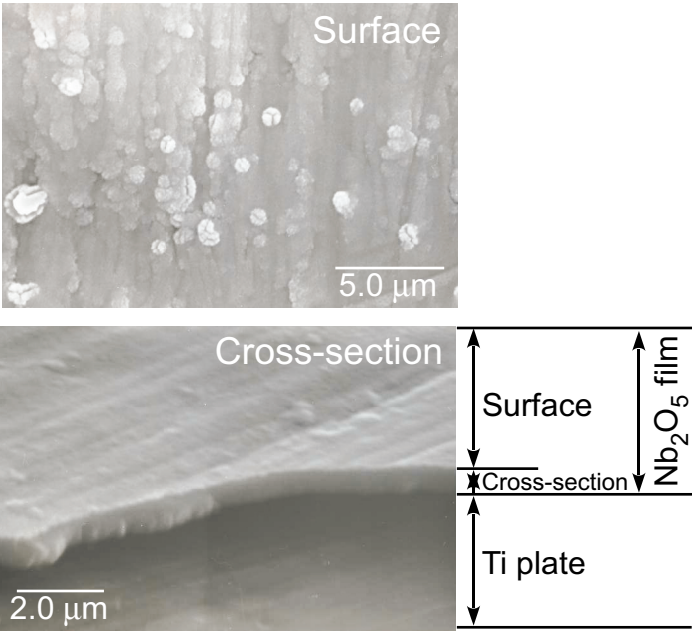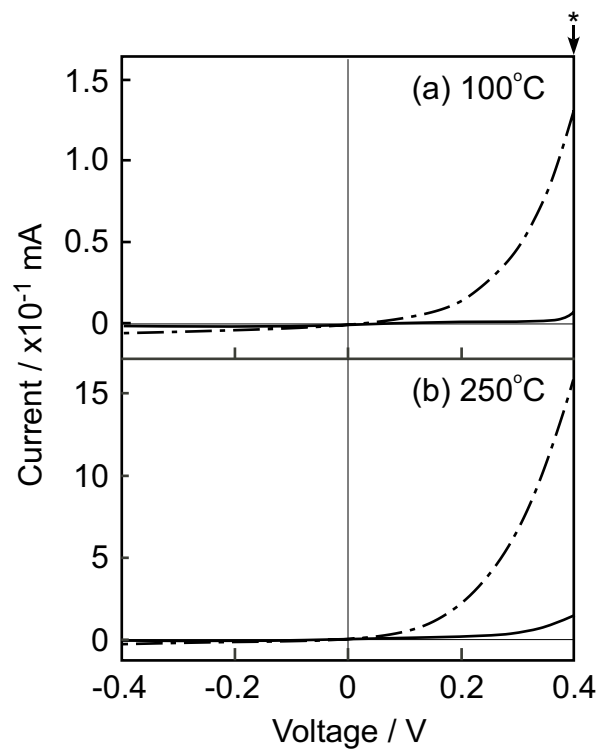
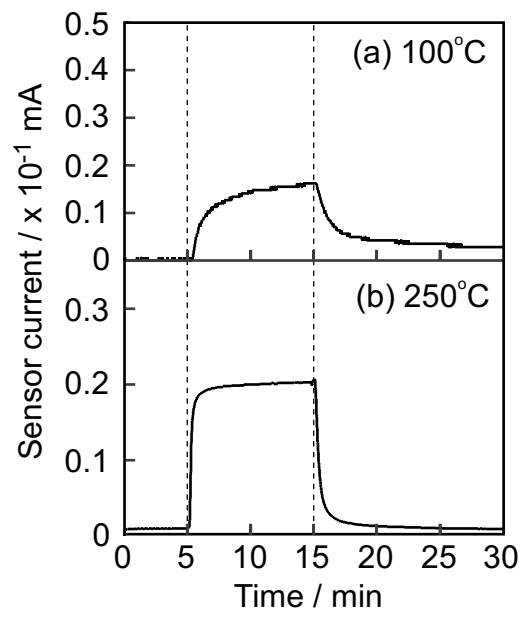Fig. 2.　Hyodo et al.

Fig. 3. Hyodo et al.

Fig. 4.   Hyodo et al.

Fig. 5.　Hyodo et al.

(a) 400°C

5.0 μm

(b) 450°C

5.0 μm

(c) 500°C

5.0 μm

(d) 550°C

5.0 μm
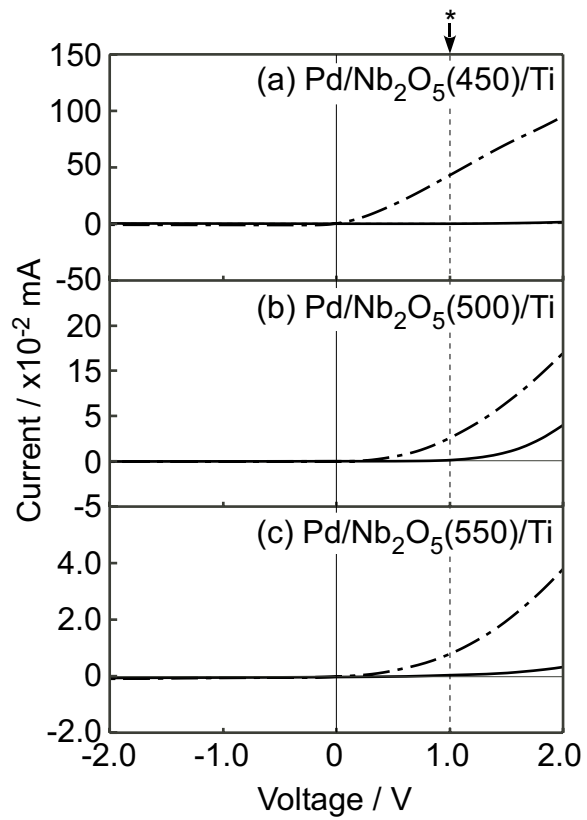
Fig. 6.   Hyodo et al.

Fig. 7.   Hyodo et al.

Fig. 8. Hyodo et al.

(a) 450°C

Surface

Cross-section

Nb plate

Surface (Nb$_2$O$_5$)

Nb$_2$O$_5$ film

20 µm

(b) 500°C

Surface

Cross-section

Nb plate

Nb$_2$O$_5$ film

20 µm

(c) 550°C

Surface

Cross-section

Nb plate

Nb$_2$O$_5$ film

20 µm
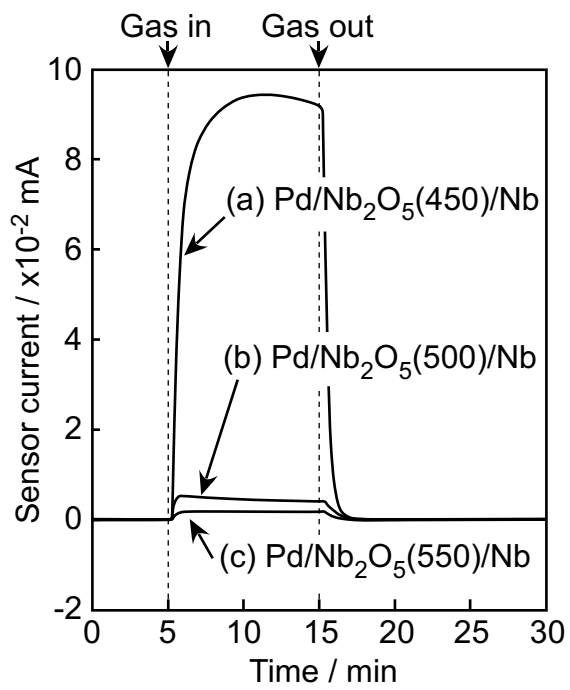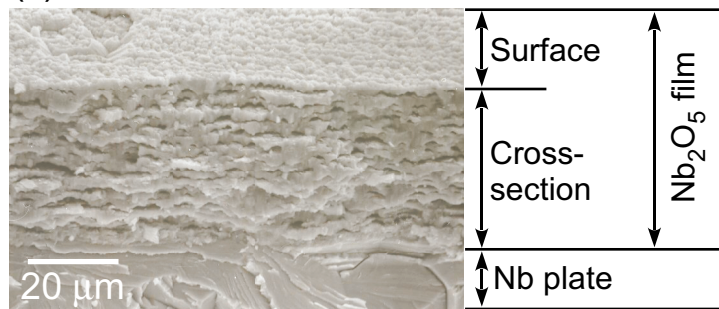
Fig. 9.   Hyodo et al.

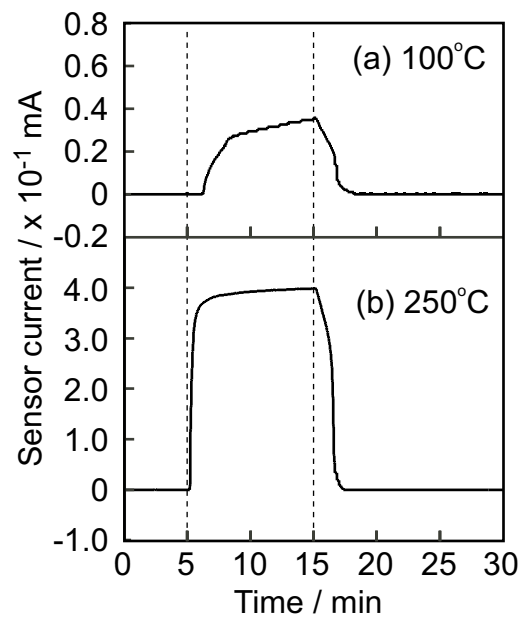Fig. 10.   Hyodo et al.

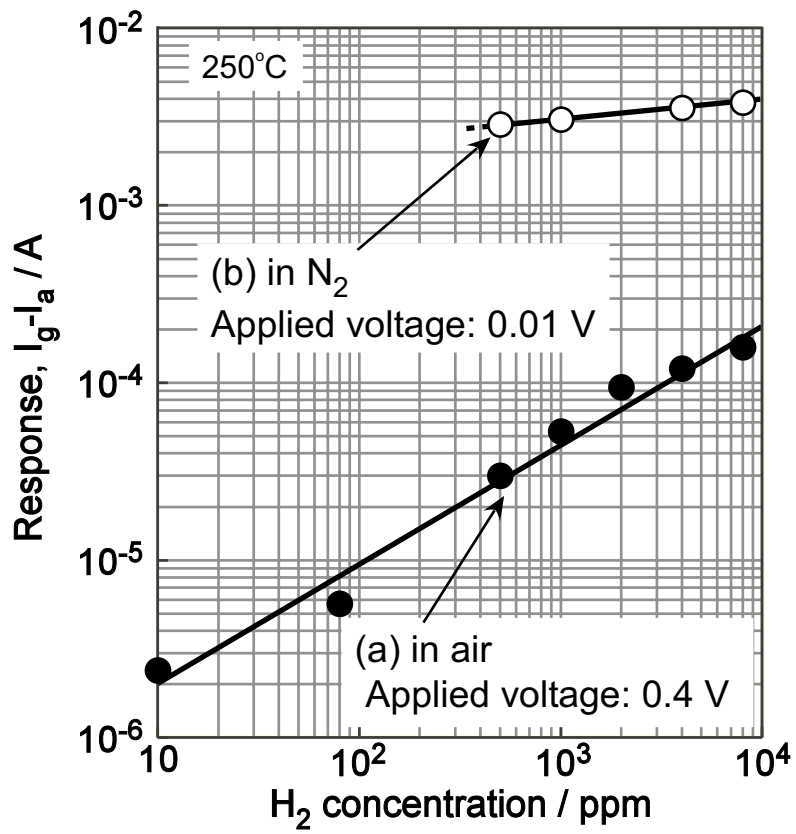Fig. 11.   Hyodo et al.

Fig. 12. Hyodo et al.

Fig. 13.　Hyodo et al.

Fig. 14.   Hyodo et al.